

Fully automated morphological analysis of patients with obstructive sleep apnea

Oktay ALĞIN^{1*}, Burak AKIN², Gökhan OCAKOĞLU³, Evrim ÖZMEN⁴

¹Department of Radiology, Atatürk Training and Research Hospital, Bilkent, Ankara, Turkey

²Department of Diagnostic Radiology, University Hospital Freiburg, Freiburg, Germany

³Department of Biostatistics, Faculty of Medicine, Uludağ University, Bursa, Turkey

⁴Department of Radiology, Cerrahpaşa Faculty of Medicine, İstanbul University, İstanbul, Turkey

Received: 30.08.2014 • Accepted/Published Online: 06.07.2015 • Final Version: 17.02.2016

Background/aim: Obstructive sleep apnea syndrome (OSAS) is a disease characterized by episodic hypoxia. We aimed to use the Freesurfer program for global evaluation of morphological changes in OSAS patients.

Materials and methods: Three-dimensional T1-weighted images were obtained, and intracranial morphology was assessed in 18 patients with OSAS and 20 controls. Results of the volume and the cortical thickness analyses of both groups were compared statistically.

Results: The total cortical, left–right hemispheres gray matter (GM), corpus callosum, and total GM volumes were lower in OSAS patients when compared with the control group ($P < 0.001$). The average cortical thickness was lower in OSAS patients bilaterally in pars orbitalis, paracentral, rostral middle frontal, middle frontal, orbital, and superior frontal gyri when compared with the control group ($P < 0.05$). Furthermore, the volume and average cortical thickness of multiple anatomic regions, apart from the brain parts mentioned above, were decreased unilaterally (e.g., hippocampus, cingulum, putamen, thalamus) in OSAS patients ($P < 0.05$).

Conclusion: Multiple morphologic changes occur in the cerebral structures of OSAS patients due to intermittent ischemia episodes. Detection of those areas with Freesurfer is easier. New studies with large series would be needed for these subjects.

Key words: Obstructive sleep apnea syndrome (OSAS), MRI, hypoxia, brain volume, voxel-based morphometry, image analysis

1. Introduction

Obstructive sleep apnea syndrome (OSAS), which is the sleep disorder most often referred to the sleep laboratories for polysomnography recording, is characterized by intermittent complete (apnea) or partial (hypopnea) obstruction episodes of the upper airway that may repeat all night long (1). The prevalence of OSAS is 1%–4% in middle-aged adults and 24%–30% in the elderly (2). There are two main symptoms in OSAS patients as follows: nocturnal symptoms during sleep (e.g., loud snoring, choking during sleep, abnormal motor activities) and daytime symptoms (e.g., intense daytime lethargy, poor memory, personality changes, hyperactivity in children) (2–4).

Although morphological and neurochemical–structural changes associated with cognitive impairment might occur due to sleep fragmentation and chronic cerebral hypoxia episodes that can lead to brain damage, the pathophysiology of the cognitive deficits is still unclear (5,6). Affected areas mostly lead to deficiency of attention, learning, memory, executive, and intellectual functioning (4).

Although routine magnetic resonance (MR) imaging (MRI) is often sufficient to show obvious cerebral injury, advanced and quantitative MRI techniques such as MR spectroscopy (MRS) and diffusion tensor imaging (DTI) can reveal neurochemical and structural changes in damaged brain tissue in OSAS patients (5,7,8). Manual, semiautomated, and automated voxel-based morphometry (VBM) methods, which have been increasingly used since 1995, provide volume and thickness calculation of the gray matter (3,4,9). Gray matter thickness and volume changes are observed in normal aging and many diseases, including Alzheimer disease and other dementias, Huntington disease, corticobasal degeneration, amyotrophic lateral sclerosis, schizophrenia, and OSAS (4,10).

Freesurfer is a fully automatic software that is primarily used in cortical parcellation and subcortical segmentation (8). This program makes reconstructions by using 3-dimensional (3D) T1-weighted (W) anatomical scans. To the best of our knowledge, there has been no previous report in the literature that evaluates the changes of all intracranial structures in OSAS patients by using

* Correspondence: droktayalgin@gmail.com

software that is able to perform fully automatic and detailed segmentation–parcellation as Freesurfer does. The aim of this study was to use a fully automated program for evaluation of the morphological changes of certain brain structures in two groups (OSAS patients and controls). With this purpose, MR images of OSAS patients and the control group were analyzed with Freesurfer software, and the data obtained using this software were compared statistically.

2. Materials and methods

2.1. Patient population

Twenty-four OSAS patients who were referred to our radiology department during the 3-year period were included in this retrospective study. The diagnosis of OSAS for each patient was obtained with polysomnography (PSG) based on the guidelines of the American Electroencephalographic Society and Epworth Sleepiness Scale (5,11). Most of our patients have new-onset OSAS. Twenty-six volunteers without any neurological sleep abnormalities, OSAS findings, or additional illnesses were included in the control group. Their neurological examinations and cranial MRI results were normal. There was no history or diagnosis of sleep disorders in the control group. Patients who suffered from trauma, malignancy, intracranial mass, cerebral ischemia or infarction, dementia, major cardiovascular disorder, or psychiatric diseases were excluded. There was no known comorbidity (hypertension, diabetes, etc.) among control subjects.

In order to avoid a possible false analysis, we excluded 4 controls and 6 OSAS patients in whom magnetization-prepared rapid acquisition gradient-echo (MPRAGE) sequence had aliasing artifacts. As a result, 18 OSAS patients (13 males, 5 female; mean age: 50 ± 9 years) and 20 control subjects (9 males, 11 females; mean age: 44 ± 9 years) were included in this study. The study was approved by the ethical committee.

2.2. MRI examinations

MR images were obtained using a 1.5-T MR unit (Magnetom Vision Plus, Siemens, Erlangen, Germany). After acquisition of scout images, sagittal plane 3D T1W data were obtained using an MPRAGE sequence (TR/TE: 9.7/4 ms; TI: 300 ms; echo train: 1; field of view: 270×270 mm; matrix: 200×256 ; number of slices: 128; slice thickness: 1.2 mm; FA: 12° ; time of acquisition: 5 min). Mean imaging time for MR evaluation was 10 min. The parameters of the MPRAGE sequence were the same for the OSAS and control subjects.

3. Data analysis

The anatomic images that were obtained from the MPRAGE sequence in DICOM format were transferred to a Linux-based computer with Freesurfer v5.0 (MGH,

Boston, MA, USA) software. First, minimal shifts caused by patient movements during the examination were corrected on the images. The MPRAGE images were then placed on the Talairach brain coordinate system (12). The brightness variations caused by the alterations of B1 magnetic field were corrected and normalized. All the white matter brightness was set at the value of 110. All of the evaluated brains were constructed on the icosahedron (20-faced polyhedron) template by using the skull-stripping procedure. Modifications in shape were made with two different forces (force and curvature reducing force) (13). Therefore, the cortical borders were determined more efficiently. White matter tagging was then done according to the brightness values. The subcortical spaces were filled and the brainstem was removed from the images to create segmentation and to generate cortex surface; thus, the white matter template was created. The brain surface model was formed with the MESH (finite element) technique. The remaining parts, including cerebrospinal fluid and brain parenchyma, were used as a brain mask during the tagging and segmentation procedures.

Automatic tagging and segmentation processes were done with the proposed method for subcortical regions; they were performed with the Destrieux template for the cortical regions (14,15) (Figure). Using the present brain template allowed us to perform the pretagging process, increased the success of segmentation, and reduced the errors caused by pathological conditions. The failed parts were corrected manually, and volume measurements were repeated by a biomedical engineer (B.A.) who is a professional Freesurfer user. Moreover, the brain

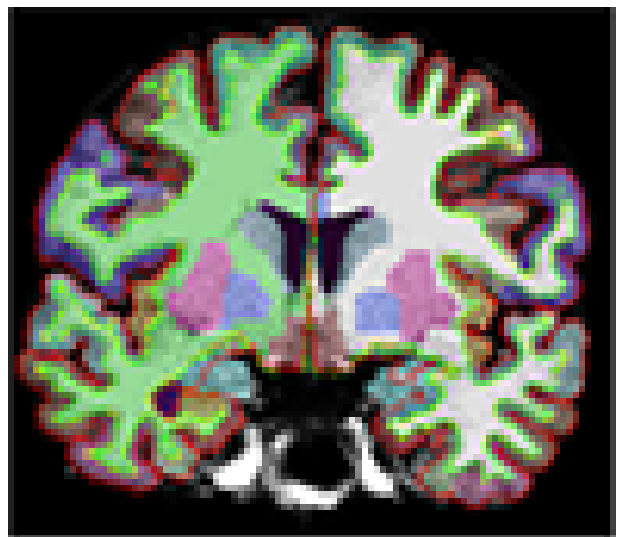


Figure. Cortical parcellation map of a control subject constructed with Freesurfer. Each cortical section was labeled with a different color tag. Deep gray matter structures and white matter of both hemispheres were fragmented and marked separately.

volume measurements obtained from every patient were normalized by dividing their own brain volume, and these results were analyzed statistically. Additional information regarding morphologic analysis using Freesurfer software can be found in references 8 and 15, and at <http://surfer.nmr.mgh.harvard.edu/fswiki/freesurferwiki>.

4. Statistical analysis

All statistical analyses were performed using SPSS 20.0 software (SPSS Inc., Chicago, IL, USA). Continuous variables are represented by median (minimum–maximum) values. For continuous variables, comparisons

of the two groups were performed by using a Mann–Whitney U test, while categorical variables were compared between groups by using a chi-square test. The level of statistical significance was set at $P < 0.05$.

5. Results

The average cortical thickness was lower in OSAS patients bilaterally at the pars orbitalis, paracentral, rostral middle frontal, frontal middle, orbital, and superior frontal gyri areas when compared with the control group subjects ($P < 0.05$) (Table 1). Similarly, the average cortical thicknesses of inferior parietal, medial orbitofrontal, precuneus, frontal

Table 1. Statistically significant average cortical thickness measurements (mm) of control and patient groups.

Right hemisphere	Controls			Patients with OSAS			P-value
	Median	Min	Max	Median	Min	Max	
Inferiorparietal	2.51	2.10	2.77	2.36	2.24	2.89	0.006
Medial orbito–frontal	2.56	2.26	2.80	2.41	2.24	2.65	0.001
Paracentral	2.25	1.86	2.58	2.16	1.83	2.48	0.035
Pars orbitalis	2.80	2.22	3.14	2.57	2.32	2.84	0.002
Precuneus	2.42	1.94	2.60	2.18	1.99	2.70	0.017
Rostral middle frontal	2.47	2.15	2.70	2.33	2.00	2.53	0.004
Superior frontal	2.76	2.36	2.99	2.62	2.35	2.95	0.012
G front middle	2.67	2.25	2.87	2.54	2.00	2.98	0.044
G front superior	2.86	2.37	3.12	2.66	2.29	3.05	0.016
G occipital middle	2.61	2.30	2.99	2.47	2.33	3.26	0.013
G orbital	2.92	2.48	3.14	2.71	2.31	2.98	0.048
G postcentral	2.07	1.48	2.31	1.93	1.49	2.36	0.044
G rectus	2.76	2.30	3.06	2.49	2.08	2.74	<0.001
G subcallosal	2.75	1.96	3.48	2.55	2.05	2.82	0.035
Left hemisphere	Median	Min	Max	Median	Min	Max	P-value
Entorhinal	3.38	2.48	3.94	3.36	2.81	3.72	0.013
Fusiform	2.65	2.45	2.92	2.58	2.37	2.85	0.016
Inferior temporal	2.86	2.64	3.17	2.85	2.51	3.30	0.041
Lateral occipital	2.22	2.03	2.49	2.15	1.91	2.48	0.033
Paracentral	2.21	1.99	2.55	2.08	1.65	2.55	0.002
Pars opercularis	2.58	2.34	2.88	2.39	1.99	2.69	0.019
Pars orbitalis	2.81	2.33	3.15	2.57	2.21	3.13	0.019
Postcentral	2.02	1.72	2.28	1.95	1.74	2.32	0.009
Precentral	2.30	1.84	2.67	2.25	1.80	2.68	0.022
Rostral anterior cingulate	2.90	2.39	3.42	2.83	2.59	3.22	0.017
Rostral middle frontal	2.47	2.05	2.75	2.35	2.07	2.60	0.033
Superior frontal	2.77	2.37	3.07	2.70	2.37	3.05	0.033
Superior temporal	2.70	2.35	2.97	2.63	2.47	2.89	0.015
G cuneus	1.81	1.51	2.21	1.68	1.55	2.08	0.006
G front middle	2.69	2.14	2.98	2.53	2.04	2.88	0.038
G orbital	2.80	2.49	3.17	2.63	2.44	3.06	0.009
G pariet inf angular	2.72	2.33	2.95	2.57	2.17	2.93	0.009
G precentral	2.44	1.89	2.79	2.43	1.72	2.86	0.038

superior, occipital middle, postcentral, rectus, gyri, and subcallosal gyri in the right hemisphere, and entorhinal, fusiform, lateral occipital, pars opercularis, superior temporal, inferior temporal, precentral, postcentral, rostral anterior cingulate, cuneus, transverse temporal, insula, occipital temporal medial parahippocampal, and parietal inferior angular gyri in the left hemisphere were unilaterally lower in the OSAS group when compared with the control group ($P < 0.05$) (Table 1).

In volumetric analysis, the total cortical ($P < 0.05$), left/right hemispheres' gray matter (GM) ($P < 0.001$), total GM ($P < 0.001$), subcortical GM ($P < 0.05$), corpus callosum ($P < 0.05$), and bilateral ventral DC–thalamus proper ($P < 0.05$) volumes were lower in OSAS patients when compared with the control group (Table 2). Likewise, normalized volume measurements of the putamen, hippocampus, accumbens area, and caudal anterior cingulate in the right hemisphere, and medial orbitofrontal, caudate, posterior cingulate, and pallidum in the left hemisphere were unilaterally lower in the OSAS group when compared with the control group ($P < 0.05$) (Table 2).

There was no significant difference between the patient and control groups in terms of cerebellar cortex or white matter volumes ($P > 0.05$). Significantly increased volume and surface area values in the left posterior cingulate cortex were observed in patients with OSAS compared with the controls ($P < 0.05$).

6. Discussion

Intermittent cerebral ischemia secondary to repeated apnea and hypopnea episodes and sleep fragmentation during sleep in OSAS patients causes several changes in the central nervous system (16,17). Emotional–cognitive changes and daytime sleepiness are the daytime symptoms of OSAS patients (11). Structural–metabolic alterations in some regions of the brain are responsible for those symptoms (18). However, the pathophysiology of OSAS is complicated and has not been completely understood yet (16). In the current retrospective study, we aimed to determine possible morphological changes of OSAS patients' brains by using fully automated analysis software (Freesurfer).

Table 2. Statistically significant differences of normalized volumetric analysis of the study population.

Volumes	Controls (mm ³)			Patients with OSAS (mm ³)			P-value
	Median	Min	Max	Median	Min	Max	
Left hemisphere cortical GM	152,784	128,459	254,542	139,037	119,714	173,430	<0.001
Right hemisphere cortical GM	155,709	128,878	256,524	141,135	119,618	170,732	<0.001
Total cortical GM	308,264	257,337	511,065	280,319	239,332	344,162	<0.001
Subcortical GM	128,323	104,816	215,524	117,585	105,102	141,501	0.044
Total GM	434,797	372,015	726,589	401,694	344,434	485,663	<0.001
Left thalamus proper	5247	4098	8107	4569	3962	5871	0.005
Left caudate	2313	1749	4308	2151	1446	2822	0.017
Left putamen	3625	3034	6734	3266	2611	3870	<0.001
Left pallidum	1100	967	2028	1041	737	1192	0.026
Left ventral DC	3028	2350	5238	2677	2343	3283	0.009
Left medial orbitofrontal	5350	4462	6067	4877.5	4239	5785	0.019
Left G rectus	1817	1399	2272	1623.5	1382	1899	0.007
Right hippocampus	2936	2559	5119	2683	2242	3242	0.003
Right accumbens area	369	292	519	316	222	481	0.026
Right ventral DC	2939	2414	4786	2614	2073	3067	0.008
Right thalamus proper	5136	3928	8799	4529	3699	5676	0.001
Right putamen	3492	2779	6130	3114	2594	3998	<0.001
CC posterior	672	471	1005	531	440	809	<0.001
CC middle posterior	321	240	511	270	194	377	0.007
CC central	342	245	550	291	217	396	0.008
CC middle anterior	346	254	590	296	199	477	0.004
CC anterior	604	496	984	491	342	726	<0.001

In this study, we used the T1W 3D-MPRAGE sequence for cerebral parcellation–segmentation since this sequence could provide excellent white and gray matter distinction. Most of the cortical and subcortical structures can be easily distinguished with this feature (8). Most of the brain structures can be analyzed by using a fully automated program (e.g., Freesurfer) without the need for drawing the region of interest manually. The Freesurfer program could save time significantly with this feature when compared with manual or semiautomated programs (8,15). In addition, volumes and cortical thicknesses of the various cerebrospinal-fluid-containing spaces and/or gray and white matter structures can be determined by using the Freesurfer program (19). In this program, approximately 8 patients could be analyzed in a day depending on the capacity of the computer used. Detection of those areas with Freesurfer is much easier than using other nonfully automated programs (12–15).

In the current study, a decrease in the average cortical thickness was detected particularly at the gyri of the frontal, parietal, and temporal lobes in the OSAS group when compared with the control group. These data are consistent with the literature (3,4,11). It is suggested in the literature that the involvement of these areas is the result of neuronal damage depending on intermittent hypoxia (2,6). Although the cause of the involvement of these regions is not clear, these areas are suggested to be more sensitive to hypoxia (2,20). However, we did not detect any significant volumetric decrease in some cortical gyri of those lobes mentioned above. Gray matter volume loss is associated with severity of the disease in OSAS patients (2,21). Most of our study patients consisted of newly diagnosed OSAS patients, which could be the reason for this situation.

We detected decreased left–right hemisphere cortical GM, total cortical GM, subcortical GM, total GM, basal ganglia, and corpus callosum volumes after volumetric analysis in OSAS patients when compared with the control group (Table 2). As reported in the literature, our data indicate the development of global or multifocal brain atrophy and/or statistically significant gray matter volume deficits in OSAS patients (2–6). Additionally, global volume reduction of the corpus callosum might be an important indicator of hypoxic white matter impairment in OSAS (22–24). Interestingly, there was no significant difference between the patient and control groups in terms of cerebellar cortex or cerebellar white matter volumes.

In our study, a unilateral decrease in the values of cortical thickness of some regions (especially the right superior frontal and left temporal lobes) was detected after the cortical parcellation (Table 1). These changes may be related to the memory impairment observed in OSAS (22–24). It has also been reported that the involvement of the regions mentioned above contributes to the symptoms (such as motor regulation imbalance and cognitive

impairment) of OSAS patients (3,4,6,11). We observed significantly increased volume and surface area values in the left posterior cingulate cortex in patients with OSAS compared with the controls. These changes might be responsible for cognitive changes (25,26).

It is reported that the involvement of the hippocampus is particularly seen in severe OSAS patients (3,4,21). However, there are some studies suggesting that there is no hippocampus abnormality in early OSAS patients (5,6,21,22). Morrell et al. detected unilateral hippocampus involvement in 7 newly diagnosed OSAS patients (2). Sarma et al. reported that significant NAA/Cr differences in the left hippocampus were observed between patients with OSAS and controls (23). In this study, we did not find prominent bilateral hippocampal involvement. However, there was also a statistically significant reduction in the right hippocampus volumes and left entorhinal cortex of the patient group (Tables 1 and 2). This could be related to our patient group consisting of newly diagnosed individuals, or our relatively small number of study cases. We suggest that hippocampal involvement could be demonstrated more optimally by using the 3D-T1W data, which consist of smaller isotropic voxels with high tesla MR devices.

There are some limitations to our study. The most important one is the relatively small number of the OSAS group. There are many factors that could lead to differences in morphometric features of the brain (age, smoking, hypertension, sex, drinking, handedness, diabetes, severity and onset of OSAS, etc.). The patient and control groups in our study were not matched for all of these factors. Furthermore, some of the controls reported having nonspecific headache. This may be a drawback. As observed in our study, a perfusion study by Innes et al. demonstrated that there was significant involvement in the paracingulate–cingulate cortex, left putamen, right hippocampus, and right thalamus (26). Another limitation of this study is that we could not assess the perfusion changes of the regions using additional techniques (such as perfusion W MR imaging), because these regions had a tendency to disparity in patients with OSAS. In addition, the achievement of 3D-T1W images used for automated parcellation with a 1.5-T MR device is the other potential limitation, as mentioned above. Since our study was retrospective, unfortunately we could not prevent these limitations. This manuscript presents only a comparison between fully automated segmentation results for OSAS patients and control subjects. Therefore, comprehensive new studies with large series are necessary to avoid these limitations and to get more effective results.

In conclusion, morphologic changes might occur in the brain and cerebrospinal fluid-containing spaces of OSAS patients due to intermittent ischemia episodes. We detected reduced gray matter concentration, specifically in

the right superior frontal gyrus, left temporal lobe, corpus callosum, basal nuclei, and right hippocampus. Freesurfer may be a useful tool for the evaluation of the cerebral changes related to OSAS. Detection of those areas with Freesurfer is very easy. New studies with large series would be required on this topic.

References

- Chokroverty S. Sleep and its disorders (chapter 72). In: Chokroverty S, editor. *Sleep Disorders Medicine: Basic Science, Technical Considerations, and Clinical Aspects*. 3rd ed. Philadelphia, PA, USA: Elsevier/Butterworth; 2009.
- Morrell MJ, McRobbie DW, Quest RA, Cummin AR, Ghiassi R, Corfield DR. Changes in brain morphology associated with obstructive sleep apnea. *Sleep Med* 2003; 4: 451–454.
- Macey PM, Henderson LA, Macey KE, Alger JR, Frysinger RC, Woo MA, Harper RK, Yan-Go FL, Harper RM. Brain morphology associated with obstructive sleep apnea. *Am J Respir Crit Care Med* 2002; 166: 1382–1387.
- Torelli F, Moscufo N, Garreffa G, Placidi F, Romigi A, Zannino S, Bozzali M, Fasano F, Giulietti G, Djonlagic I et al. Cognitive profile and brain morphological changes in obstructive sleep apnea. *Neuroimage* 2011; 54: 787–793.
- Algin O, Gokalp G, Ocakoglu G, Ursavas A, Taskapilioglu O, Hakyemez B. Neurochemical–structural changes evaluation of brain in patients with obstructive sleep apnea syndrome. *Eur J Radiol* 2012; 81: 491–495.
- O'Donoghue FJ, Briellmann RS, Rochford PD, Abbott DF, Pell GS, Chan CH, Tarquinio N, Jackson GD, Pierce RJ. Cerebral structural changes in severe obstructive sleep apnea. *Am J Respir Crit Care Med* 2005; 171: 1185–1190.
- Davies CW, Crosby JH, Mullins RL, Traill ZC, Anslow P, Davies RJ, Stradling JR. Case control study of cerebrovascular damage defined by magnetic resonance imaging in patients with OSA and normal age-matched control subjects. *Sleep* 2001; 24: 715–720.
- Fjell AM, Westlye LT, Greve DN, Fischl B, Benner T, van der Kouwe AJW, Salat D, Bjørnerud A, Due-Tønnessen P, Walhovd KB. The relationship between diffusion tensor imaging and volumetry as measures of white matter properties. *Neuroimage* 2008; 42: 1654–1668.
- Wright J, Sheldon TA, Watt I. Sleep apnea. *Lancet* 1999; 354: 600.
- Fischl B, Dale AM. Measuring the thickness of human cerebral cortex from magnetic resonance images. *Proc Natl Acad Sci USA* 2000; 275: 30864–30872.
- Alchanatis M, Deligiorgis N, Zias N, Amfilochiou A, Gotsis E, Karakatsani A, Papadimitriou A. Frontal brain lobe impairment in obstructive sleep apnea: a proton MR spectroscopy study. *Eur Respir J* 2004; 24: 980–986.
- Collins DL, Neelin P, Peters TM, Evans AC. Automatic 3D intersubject registration of MR volumetric data in standardized Talairach space. *J Comput Assist Tomogr* 1994; 18: 192–205.
- Dale AM, Fischl B, Sereno MI. cortical surface-based analysis. I. Segmentation and surface reconstruction. *Neuroimage* 1999; 9: 179–194.
- Fischl B, Salat DH, Busa E, Albert M, Dieterich M, Hasalgrove C, van der Kouwe A, Killiany R, Kennedy D, Klaveness S et al. Whole brain segmentation: automated labeling of neuroanatomical structures in the human brain. *Neuron* 2002; 33: 341–355.
- Destrieux C, Fischl B, Dale A, Halgren E. Automatic parcellation of human cortical gyri and sulci using standard anatomical nomenclature. *Neuroimage* 2010; 53: 1–15.
- Desseilles M, Dang-Vu T, Schabus M, Sterpenich V, Maquet P, Schwartz S. Neuroimaging insights into the pathophysiology of sleep disorders. *Sleep* 2008; 31: 777–794.
- Engleman H, Joffe D. Neuropsychological function in obstructive sleep apnea. *Sleep Medicine Reviews* 1999; 3: 59–78.
- Zimmerman ME, Aloia MS. A review of neuroimaging in obstructive sleep apnea. *J Clin Sleep Med* 2006; 130: 1772–1778.
- Desikan RS, Segonne F, Fischl B, Quinn BT, Dickerson BC, Blacker D, Buckner RL, Dale AM, Maguire RP, Hyman BT et al. An automated labeling system for subdividing the human cerebral cortex on MRI scans into gyral based regions of interest. *Neuroimage* 2006; 31: 968–980.
- Kamba M, Suto Y, Ohta Y, Inoue Y, Matsuda E. Cerebral metabolism in sleep apnea: evaluation by magnetic resonance spectroscopy. *Am J Respir Crit Care Med* 1997; 156: 296–298.
- Giulietti G, Torelli F, Bozzali M, Garreffa G, Muscofo N, Zannino S, Serra L, Placidi F, Fasano F, Hagberg G et al. Brain structural changes underlying cognitive disabilities in patients with obstructive sleep apnea syndrome (OSAS): a VBM study. *Proc ISMRM* 18, 2010: 2417.
- Kızılgöz V, Aydın A, Tatar IG, Hekimoğlu B, Ardiç S, Fırat H, Dönmez C. Proton magnetic resonance spectroscopy of periventricular white matter and hippocampus in obstructive sleep apnea patients. *Pol J Radiol* 2013; 78: 7–14.
- Sarma MK, Nagarajan R, Macey PM, Kumar R, Villablanca JP, Furuyama J, Thomas MA. Accelerated echo-planar J-resolved spectroscopic imaging in the human brain using compressed sensing: a pilot validation in obstructive sleep apnea. *AJNR Am J Neuroradiol* 2014; 35: S81–S89.
- Weng HH, Tsai YH, Chen CF, Lin YC, Yang CT, Tsai YH, Yang CY. Mapping gray matter reductions in obstructive sleep apnea: an activation likelihood estimation meta-analysis. *Sleep* 2014; 37: 167–175.
- Leech R, Sharp DJ. The role of the posterior cingulate in cognition and disease. *Brain* 2014; 137: 12–32.
- Innes CR, Kelly PT, Hlavac M, Melzer TR, Jones RD. Decreased regional cerebral perfusion in moderate–severe obstructive sleep apnoea during wakefulness. *Sleep* 2015; 38: 699–706.

Acknowledgments

The authors thank Prof Ergin Atalar and Prof Gökhan Gokalp for their contributions. A part of this study was presented at the 28th European Society for Magnetic Resonance in Medicine and Biology Annual Meeting held in Leipzig, Germany on 18–21 October 2011.